von Neumann entropy and on-site localization for perpetually coupled qubits

Kingshuk Majumdar*
Department of Physics, Grand Valley State University, Allendale, Michigan 49401, USA
(Received 23 November 2008; published 30 March 2009)

We use the von Neumann entropy to study the single- and many-particle on-site localizations of stationary states for an anisotropic Heisenberg spin-$\frac{1}{2}$ chain. With a constructed bounded sequence of on-site energies for single- and many-particle systems we demonstrate that the von Neumann entropy approaches zero, indicating strong on-site localizations for all states. On the contrary, random on-site energy sequence does not lead to strong on-site confinement of all states. Our numerical results indicate that the von Neumann entropy provides insight to analyze on-site localizations for these systems.

DOI: 10.1103/PhysRevB.79.115134 PACS number(s): 03.67.Lx, 72.15.Rn, 75.10.Pq, 73.23.−b

I. INTRODUCTION

Following the seminal work of Anderson[1,2] in 1958, disorder-induced localization became an active area of research in condensed-matter physics.[3,4] Current interest in quantum computation and quantum information processing has further revived the importance of studying localization of quantum bits or qubits.[5] In many proposed experimental realizations of a quantum computer, such as ion traps,[6] nuclear magnetic-resonance systems,[7,8] optical lattices,[9,10] and quantum dots,[11] a key common feature is the presence of qubit-qubit interaction, which is needed to perform two-qubit logical operations. The couplings of the qubits with the external environment lead to a finite lifetime to the excited state of a given qubit. In order to perform a computation an ideal quantum computer must be isolated from the outside environment and at the same time its qubits have to be accessible to perform quantum gate operations. The major challenge in realizing such a quantum computer is to obtain a delicate balance between the time for which the system remains quantum mechanically coherent, which is the decoherence time and the time it takes to perform quantum gate operations.

The interactions between qubits cannot be completely turned off in a realistic quantum computer. However, it can be controlled so that measurements can be performed on individual qubits. Recent theoretical works in this direction on many-particle systems have shown a way to achieve this.[12–14] By appropriately tuning the on-site energy levels for the qubits it has been shown that delocalization can be suppressed, which results in strong on-site confinement of all stationary states in the system. In this case the effective localization length is much smaller than the intersite distance instead of an exponential decay of the wave function over many sites.

Recently there has been a tremendous effort to understand the properties of quantum entanglement, which is one of the most intriguing features of quantum theory.[15] It plays a key role in many of the applications of quantum information processing.[5,16] Quantum entanglement measured by the von Neumann entropy has been extensively studied in various condensed-matter systems in recent years.[17] It has been found that the von Neumann entropy can be used to identify quantum phase transitions in fermionic systems[18–22] and localization-delocalization transitions in interacting electron systems.[23,24]

In this paper we explore the possibility of using the von Neumann entropy as a measure for identifying strong on-site localization for single- and many-particle systems of qubits. von Neumann entropy approach provides insight into localization, which is complementary to other approaches that have been used before especially the inverse participation ratio (IPR).[12–14] We consider localization for systems with constructed on-site and random on-site energies. For a finite system with constructed on-site energy sequence for qubits we show evidence for strong on-site localizations of *all* states using the von Neumann entropy. For the same system with random on-site energy sequence we find that it does not lead to strong on-site localization.

II. MODEL

Qubits being two-level systems can be modeled as spin-$\frac{1}{2}$ chains in a one-dimensional lattice in presence of an effective magnetic field along the z direction. The excitation energy of a qubit will then be the Zeeman energy of a spin, and the qubit-qubit interaction will be represented by the exchange spin coupling. The Hamiltonian of the anisotropic spin-$\frac{1}{2}$ chain in an effective magnetic field is

$$H = H_0 + H_1,$$

$$H_0 = \sum_{n=1}^{L} \epsilon_n S_n^z + \frac{1}{2}\sum_{n=1}^{L-1} J_{nn+1}^z S_n^z S_{n+1}^z,$$

$$H_1 = \frac{1}{2}\sum_{n=1}^{L-1} J_{nn+1}(S_n^x S_{n+1}^x + S_n^y S_{n+1}^y). \quad (1)$$

Here $J_{nn+1}^x = J_{nn+1}^y$ and J_{nn+1}^z are the exchange couplings between nearest-neighbor sites $n, n+1$. L is the number of sites and the parameter ϵ_n corresponds to the Zeeman splitting of spin n due to the static magnetic field in the z direction. We have considered J_{nn+1}^x and J_{nn+1}^y to be equal to J so that the qubit interaction terms do not oscillate at qubit transition frequencies. Using Jordon-Wigner transformation[25] the Hamiltonian for the XXZ spin chain [Eq. (1)] can be mapped onto a system of spinless interacting fermions.[26] The result-

ing Hamiltonian, expressed in terms of the fermion creation and annihilation operators ($a_n^\dagger$ and a_n), is

$$H = H_0 + H_1,$$

where

$$H_0 = \sum_{n=1}^{L} \epsilon_n a_n^\dagger a_n + J\Delta \sum_{n=1}^{L-1} a_n^\dagger a_{n+1}^\dagger a_{n+1} a_n,$$

$$H_1 = \frac{1}{2} J \sum_{n=1}^{L-1} (a_n^\dagger a_{n+1} + a_{n+1}^\dagger a_n). \tag{2}$$

Here, $J = J_{nn+1}^{xx}$ $(J>0)$ is the fermion hopping integral, $J\Delta = J_{nn+1}^{zz}$ is the interaction energy of fermions on neighboring sites, and on-site fermion energies ϵ_n represent the on-site Zeeman energies of the spins (or the excitation energies of the qubits). The dimensionless parameter Δ $(\Delta>0)$ characterizes the anisotropy of the spin-spin interaction. For the on-site fermion energies ϵ_n we have used the bounded one-parameter sequence[12] with $n \geq 1$;

$$\epsilon_n = \frac{1}{2} h \left[(-1)^n - \sum_{k=2}^{n+1} (-1)^{\mathrm{int}(n/k)} \alpha^{k-1} \right], \tag{3}$$

where h is the intersubband distance that significantly exceeds the hopping integral J and α $(0 \leq \alpha < 1)$ is a one-dimensional parameter. $\mathrm{int}(n/k)$ represents the integer part. This constructed energy sequence detunes the on-site energies ϵ_n from others. For $\alpha=0$, ϵ_n splits into two major subbands at $\pm h/2$ for even and odd values of n. For small values of α, the two major subbands have width $\approx \alpha h$ and are separated by $\approx h$. With an increase in α the subbands start overlapping and finally the separation between the subbands disappears.

To compare our results with some other on-site energy sequence we consider a simple random sequence of on-site energies;

$$\epsilon_n = W r_n, \tag{4}$$

where W is the bandwidth and r_n are n-independent random numbers uniformly distributed in the interval $[0,1]$.

For our model of spinless interacting fermions there are two possible local states at each site, $|1\rangle$ and $|0\rangle$ corresponding to the nth site being occupied by a single fermion and the site being empty. The local-density matrix at site n in eigenstate j is

$$\rho_n^j = |\psi_n^j|^2 (|0\rangle\langle 0|)_n + (1 - |\psi_n^j|^2)(|1\rangle\langle 1|)_n. \tag{5}$$

The wave function for the N-particle eigenstate is given by $|\psi_N^j\rangle = \Sigma_{k=1}^N \psi_k^j |j\rangle$. In Eq. (5), ψ_n^j is the amplitude of an energy eigenstate j at site n. The local von Neumann entropy, S_n^j, is defined as[5]

$$S_n^j = -|\psi_n^j|^2 \log_2 |\psi_n^j|^2 - (1 - |\psi_n^j|^2) \log_2 (1 - |\psi_n^j|^2). \tag{6}$$

The spectrum averaged von Neumann entropy $\langle S \rangle$ is the entropy averaged over all the eigenstates M and total number of sites N,

$$\langle S \rangle = \frac{1}{MN} \sum_{n=1}^{N} \sum_{j=1}^{M} S_n^j. \tag{7}$$

For many-particle system with L sites and N particles, the number of energy eigenstates is $M = L!/N!(L-N)!$.

One of the basic properties of the von Neumann entropy is subadditivity. For two distinct quantum systems, A and B, the joint entropy for the two systems satisfy the inequality: $S(A,B) \leq S(A) + S(B)$. The equality holds if and only if systems A and B are uncorrelated,[5] which is the case with different realizations of random on-site energies. Thus for the random on-site energy sequence [Eq. (4)] we have averaged the entropies $\langle S \rangle$ over all the different random configurations.

There are two special cases where Eq. (7) has simple analytical expressions. For an extended state j, $\psi_n^j = 1/\sqrt{N}$ for all n. Then it follows that the averaged entropy is a constant equal to

$$\langle S \rangle = -\frac{1}{MN} \log_2 \frac{1}{N} - \frac{N-1}{MN} \log_2 \left(1 - \frac{1}{N} \right). \tag{8}$$

For a localized state $\psi_n^j = \delta_{nm}$ (m is a given site), $\langle S \rangle = 0$. So the normalized $\langle S \rangle$ varies between 0 (for localized states) and 1 (for extended states).

Another quantitative measure that is widely used to characterize localization is the inverse participation ratio, I_j for eigenstate j which is defined as

$$I_j = \left(\sum_n |\psi_n^j|^4 \right)^{-1}. \tag{9}$$

For our calculations we use the inverse participation ratio averaged over all eigenstates M

$$\langle \mathrm{IPR} \rangle = \frac{1}{M} \sum_{j=1}^{M} I_j. \tag{10}$$

For fully localized states $I_j = 1$. $I_j \approx 1$ is an indicator of strong on-site localization of the jth state of the system. For extended states $I_j \gg 1$, with no upper bound.

III. NUMERICAL RESULTS

A. Single-particle localization

We consider a single-particle system with $L=100$ and $L=300$ sites. For the on-site energies we use the constructed energy sequence in Eq. (3) with the following parameters for the intersubband distance h and hopping integral J: $J = 1/30$, $h = 20J$. With h much greater than J the on-site energies are separated in two subbands for even and odd n. Next by choosing a dimensionless parameter α of the order of J/h we further split each subband into two separate bands to detune the next-nearest neighbors. We then construct the Hamiltonian in Eq. (2) and diagonalize it to obtain the energy eigenstates. Interaction energy Δ is equal to zero for the single-particle case. With these eigenstates we numerically calculate the spectrum averaged entropy $\langle S \rangle$ and the averaged inverse participation ratio $\langle \mathrm{IPR} \rangle$.

In Fig. 1 we plot $\langle S \rangle$ as a function of α for both $L=100$ and $L=300$ site chains. In the inset we show the results for

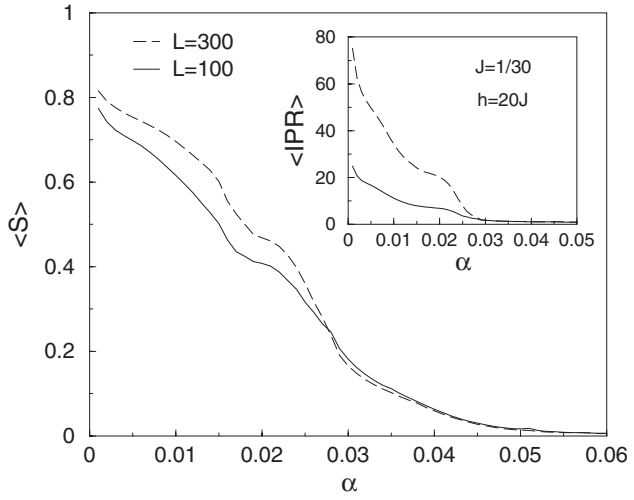

FIG. 1. Single-particle spectrum averaged von Neumann entropy $\langle S\rangle$ [normalized by the constant in Eq. (8)] is plotted for $L=100$ and $L=300$ sites as a function of a dimensionless parameter α. The constructed energy sequence [Eq. (3)] is used for the on-site energies. The hopping integral $J=1/30$ and the intersubband distance $h=20J$ is used for this plot. In the inset the average inverse participation ratio, $\langle \mathrm{IPR}\rangle$ is plotted. Both $\langle \mathrm{IPR}\rangle$ and $\langle S\rangle$ decrease with increase in α. Strong on-site localization $\langle S\rangle \to 0$ or $\langle \mathrm{IPR}\rangle \to 1$ occurs at $\alpha \approx 0.1$ for both $L=100$ and $L=300$ sites chain.

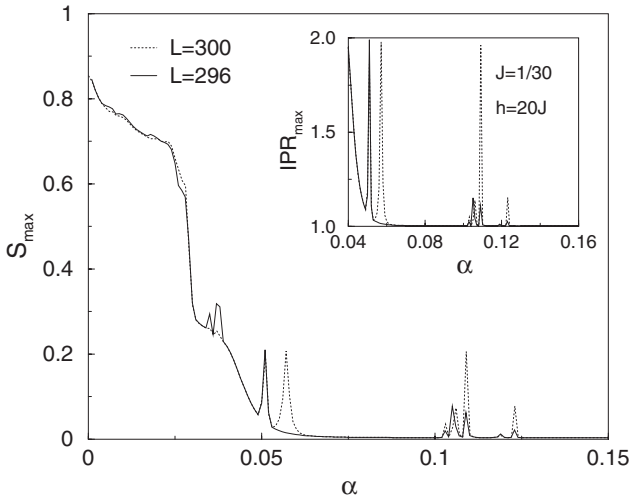

FIG. 2. Maximal single-particle von Neumann entropy $S_{\max}$ (maximal IPR in the inset) is plotted as function of α for $L=300$ and $L=296$ sites. Equation (3) has been used for the energy sequence. Both $S_{\max}$ and $\mathrm{IPR}_{\max}$ sharply decrease with increase in α showing strong on-site single-particle localization. The narrow peak for $L=300$ sites chain close to $\alpha \approx 0.1$ is due to the boundary effect. This sharp peak greatly reduces in size for $L=296$ sites chain.

the $\langle \mathrm{IPR}\rangle$. For $\alpha \to 0$ the energy sequence in Eq. (3) reduces to $\epsilon_n = (-1)^n h/2$. Hence, the stationary states form two bands of widths $\approx J^2/h$ (for $h \gg J$) centered at $\pm h/2$ for even and odd n. With increase in α, the bands at $\pm h/2$ further split into more and more subbands. This results in the monotonic decrease in both the entropy and the $\langle \mathrm{IPR}\rangle$. The spatial decay of single-particle stationary states has been studied in detail in Ref. 12 where it has been shown that strong on-site confinement of the stationary states occur as α exceeds a certain threshold value $\alpha_{\mathrm{th}} = J/2h$. Our numerical results are in good agreement with the theoretical estimate. We find $\langle S\rangle \to 0$ and $\langle \mathrm{IPR}\rangle \to 1$ for $\alpha \approx 0.1$ demonstrating strong on-site localization for all states.

Figure 2 shows that the maximal von Neumann entropy $S_{\max}$ and maximal IPR exhibit sharp resonant peaks (shown for $L=300$ and $L=296$ sites). Maximal entropy for each α is obtained from a set of averaged entropies for all the eigenstates, $S_{\max} \equiv \max_j \langle S\rangle_j$. Maximal IPR is obtained similarly, $\mathrm{IPR}_{\max} \equiv \max_j I_j$. The narrow peaks are seen for $S_{\max}$ close to zero ($\mathrm{IPR}_{\max}$ close to one), which demonstrate that very few on-site states are hybridized with each other. The resonant peak near $\alpha \approx 0.1$ is due to hopping-induced shift of energy levels of $\approx (J/2)^2/h$. For the chain with $L=296$ sites the sharp peak for $\alpha \approx 0.1$ is greatly reduced in size. In this case the shift in energy is $\approx J^2/2h$. The difference of ϵ_n for $L=300$ and $L=296$ sites is $\approx h\alpha^3$ for $\alpha \ll 1$.

The rationale for choosing the different parameters in the model is shown in Fig. 3, where we plot the von Neumann entropy as a function of α and J/h for the single-particle system with $L=100$ sites. The entropy decreases sharply with increase in α and h/J reaching a minimum value $\langle S\rangle = 0.0031$ for $\alpha = 0.166$ and $h/J = 22$. So for small α and $h/J \approx 20$ *most of the states* are locally confined on sites.

In Fig. 4 we plot the normalized probability distribution $P(S)$ and $P(I)$ (in the inset) for the random on-site energy sequence [Eq. (4)]. The probability distributions (histogram plots) are obtained by averaging the entropy and inverse participation ratio over 2000 random on-site energy configurations. Sharp peak close to $S \to 0$ or $I \to 1$ demonstrate that many of the states are localized. However, the distributions are broad and resonances are seen indicating strong hybridization between neighboring sites, which means *all the states* are not confined.

The entropy and the IPR for the constructed energy sequence differ significantly from the random on-site energy sequence. For the constructed sequence we find strong on-site localization of all states, whereas with the random sequence the confinement is not so strong.

B. Many-particle localization

In this section we investigate the on-site localization of all states for a many-particle system with $L=12$ sites and $N=6$ particles where no two particles can occupy the same site. Here we have a total number of $12!/6!6! = 924$ ways of putting six particles in 12 sites. We construct the Hamiltonian in occupation number basis states and then diagonalize the 924×924 Hamiltonian matrix to obtain the energy eigenstates.

In Fig. 5 we plot the entropy (and IPR in the inset) as a function of the dimensionless parameter α for the on-site energy sequence in Eq. (3). The entropy and the IPR have been averaged over all the 924 eigenstates. Three different values of the interaction parameter $\Delta = 0$, 0.5, and 1 are chosen for the plots. $\Delta = 0$ corresponds to only *XX*-type coupling between the nearest-neighbor spins—this case is similar to the single-particle case. The decrease in $\langle S\rangle$ with increase in

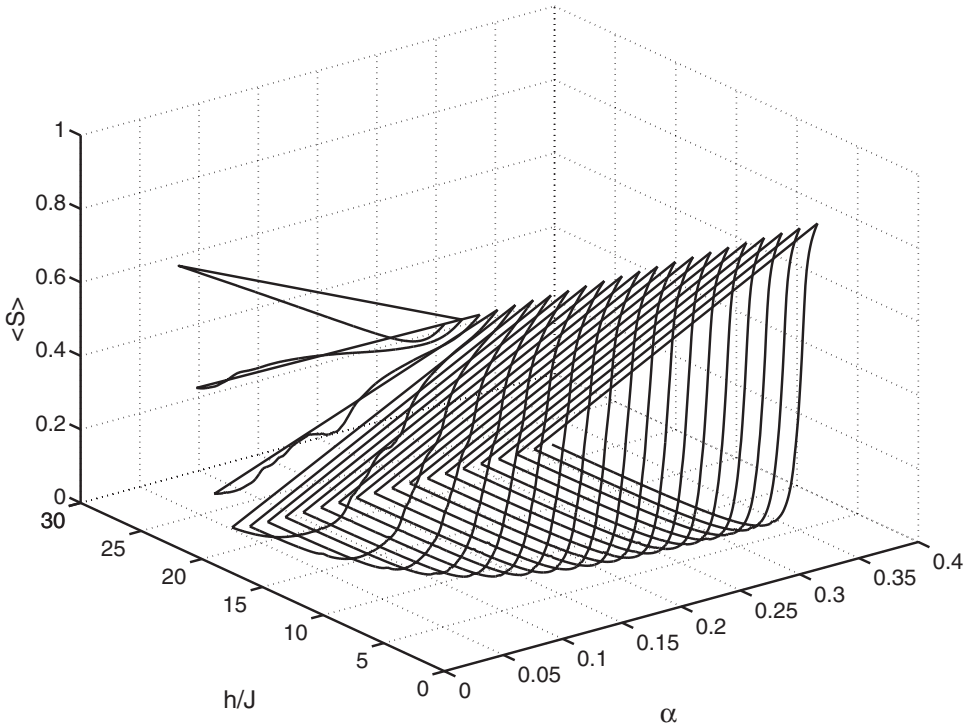

FIG. 3. Three-dimensional plot of the single-particle von Neumann entropy $\langle S\rangle$ as a function of a α and h/J for $L=100$ sites and for the energy sequence. The entropy sharply decreases with increase in α and h/J. The minimum $\langle S\rangle=0.0031$ occurs for $\alpha=0.166$ and $h/J=22$.

α is seen for all three values of Δ. Figure 6 shows the decrease in the maximal entropy and maximal IPR (in the inset) with increase in α for $\Delta=0$ and 1.

Localization of many-particle system differ from single-particle system due to the interaction term $J\Delta$ in the Hamiltonian. Figure 5 shows that the entropy (and IPR) decreases with increase in Δ. For $\Delta \gg J/h$, the energy bands at $\pm h/2$ split into subbands. Such splitting lowers the value of $\langle S\rangle$ and IPR for nonzero Δ.

For nonzero Δ, many-particle resonances are seen in Figs. 5 and 6 for small values of α, indicating some stationary states are no longer on-site localized. Strong on-site localization of the states require that the energies of the distant sites must be tuned away from each other. This happens for large values of α, where we find $\langle S\rangle$ approaches zero as $\alpha \to 0.1$

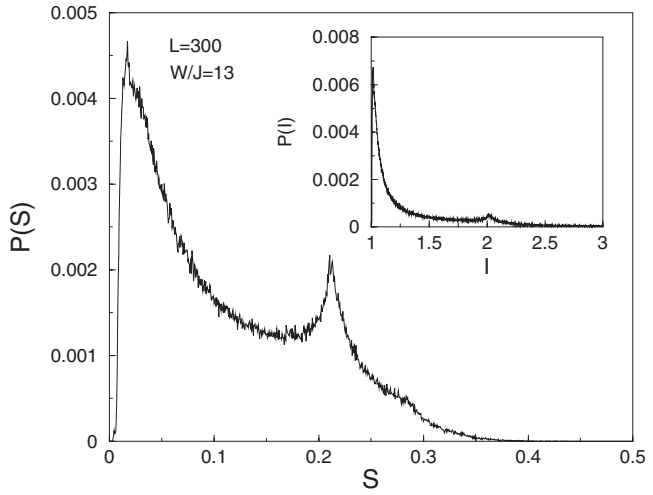

FIG. 4. Normalized single-particle probability distribution of the spectrum averaged von Neumann entropy $P(S)$ is plotted for $L=300$ sites with random energy sequence [Eq. (4)] of bandwidth $W=13J$. The entropy has been averaged over an ensemble of 2000 random on-site energy configurations. In the inset the probability distribution for the inverse participation ratio $P(I)$ is shown. The sharp peak at $S\approx 0$ (and $I\approx 1$ in the inset) is the indication of localization. However, the distributions are broad indicating strong hybridization between many sites. Multiple resonances occur due to these hybridization one of which we find for $S\approx 0.2$ or $I\approx 2$.

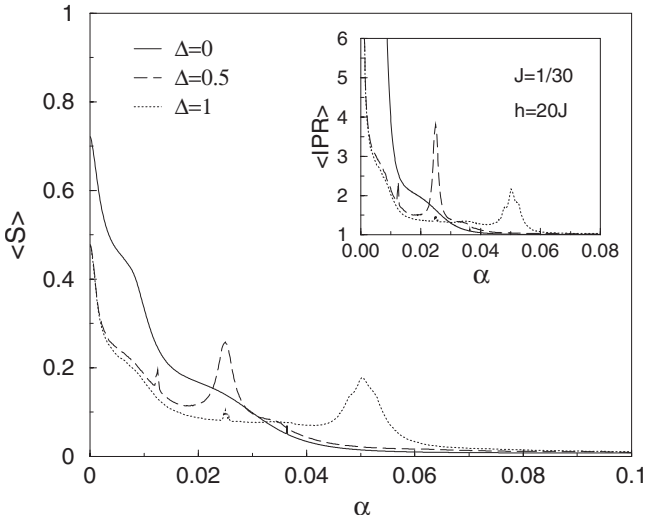

FIG. 5. Spectrum averaged von Neumann entropy for a system with $N=6$ particles in $L=12$ sites and with constructed energy sequence plotted against α. Three values of the interaction parameter $\Delta=0,0.5,1$ are used for the plots. In the inset averaged IPR is plotted. Strong on-site localization $\langle S\rangle \to 0$ or $\langle \mathrm{IPR}\rangle \to 1$ occurs for α close to 0.1 for all three values of Δ. For $\Delta \neq 0$ isolated peaks at various values of α is due to hybridization of resonating on-site many-particle states.

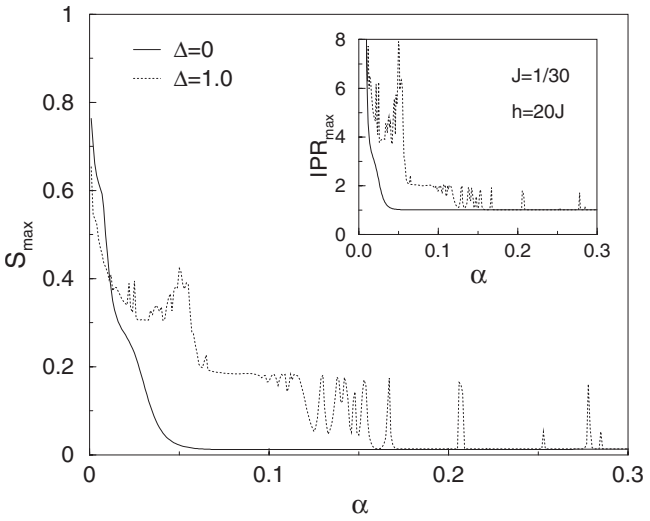

FIG. 6. Plot of maximal many-particle von Neumann entropy (maximal IPR in the inset) for $N=6$ particles in $L=12$ sites. Two values of the interaction parameter $\Delta=0,1$ are used. Both $S_{\max}$ and $\mathrm{IPR}_{\max}$ sharply decrease with increase in α showing strong on-site single-particle localization. However, sharp isolated peaks are seen for $\Delta=1.0$, which indicates that some of the stationary states are not localized on-site. These states are strongly hybridized with other resonating on-site many-particle states.

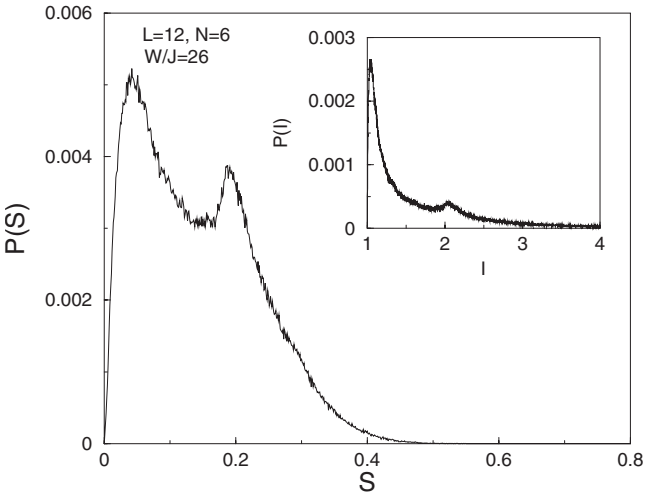

FIG. 7. Normalized probability distribution of the von Neumann entropy $P(S)$ is plotted for $N=6$ particles in $L=12$ sites with random energy sequence. Bandwidth is chosen to be $W=26J$. The entropy has been averaged over an ensemble of 2000 random on-site energy configurations. In the inset the probability distribution for the inverse participation ratio $P(I)$ is shown. The sharp peak at $S\approx 0$ (and $I\approx 1$ in the inset) is the indication of localization. However, the distributions are broad indicating strong hybridization between many sites. Peaks at $S=0.2$ or $I=2$ occur due to hybridization between many-particle states.

demonstrating strong on-site localization of all states.

Similar to the single-particle case, we calculate the three-dimensional plot of entropy as a function of α and h/J. We find that the von Neumann entropy decreases with increase in α and h/J. The minimum value of $\langle S\rangle=0.0061$ occurs for $\alpha\approx 0.23$ and $h/J\approx 22$.

Figure 7 shows the normalized probability distribution for the von Neumann entropy, $P(S)$ [normalized probability distribution for the inverse participation ratio, $P(I)$ in the inset] for the random on-site energy sequence. As before both the entropy and the IPR have been averaged over 2000 random on-site energy configurations. Peak at $S\approx 0$ shows localization of many of the states but not all. The distribution is broad, and many-particle resonances are seen (as an example the smaller peak at $S\approx 0.2$), which means that many on-site states are strongly hybridized as the stationary wave functions spread over many sites. This is in contrast to the case with constructed energy sequence where *most* of the states are strongly confined for $\alpha>0.1$.

IV. CONCLUSIONS

In this paper we have explored the use of von Neumann entropy to characterize strong on-site localization for interacting qubits. For a successful realization of a quantum computer strong on-site localization of all states is a necessity. We have considered both single- and many-particle systems with a carefully constructed sequence of on-site energies. With our numerical results we have demonstrated that von Neumann entropy approaches zero for such systems with certain values of the parameters in the model, thus indicating strong on-site localization of all states. For comparison we have studied single- and many-particle systems with random on-site energies where we find hybridization between many sites. All the sites for the random case are not confined which results in a wide probability distribution of the entropy with multiple resonance peaks.

In conclusion, we have found that the von Neumann entropy provides a systematic approach to the problem and is thus an effective tool to study localization-delocalization transitions in these many-particle interacting systems.

ACKNOWLEDGMENTS

The author gratefully acknowledges helpful discussions with M. I. Dykman. This work was supported by a grant from the Research Corporation.

*majumdak@gvsu.edu

[1] P. W. Anderson, Phys. Rev. **109**, 1492 (1958).
[2] P. W. Anderson, Proc. Natl. Acad. Sci. U.S.A. **69**, 1097 (1972).
[3] D. C. Licciardello and E. N. Economou, Phys. Rev. B **11**, 3697 (1975).
[4] P. A. Lee and T. V. Ramakrishnan, Rev. Mod. Phys. **57**, 287 (1985).
[5] M. A. Nielson and I. L. Chuang, *Quantum Computation and*

Quantum Information, 1st ed. (Cambridge University Press, Cambridge, England, 2000).
[6] J. I. Cirac and P. Zoller, Phys. Rev. Lett. **74**, 4091 (1995).
[7] N. A. Gershenfeld and I. L. Chuang, Science **275**, 350 (1997).
[8] T. D. Ladd, J. R. Goldman, F. Yamaguchi, Y. Yamamoto, E. Abe, and K. M. Itoh, Phys. Rev. Lett. **89**, 017901 (2002).
[9] G. K. Brennen, C. M. Caves, P. S. Jessen, and I. H. Deutsch, Phys. Rev. Lett. **82**, 1060 (1999).
[10] D. Jaksch, H. J. Briegel, J. I. Cirac, C. W. Gardiner, and P. Zoller, Phys. Rev. Lett. **82**, 1975 (1999).
[11] D. Loss and D. P. DiVincenzo, Phys. Rev. A **57**, 120 (1998).
[12] L. F. Santos, M. I. Dykman, M. Shapiro, and F. M. Izrailev, Phys. Rev. A **71**, 012317 (2005).
[13] M. I. Dykman, L. F. Santos, M. Shapiro, and F. M. Izrailev, Quantum Inf. Comput. **5**, 335 (2005).
[14] M. I. Dykman, L. F. Santos, and M. Shapiro, J. Opt. B: Quantum Semiclassical Opt. **7**, S363 (2005).
[15] A. Einstein, B. Podolsky, and N. Rosen, Phys. Rev. **47**, 777 (1935).
[16] C. H. Bennett and D. P. Devincenzo, Nature (London) **404**, 247 (2000).
[17] L. Amico, R. Fazio, A. Osterloh, and V. Vedral, Rev. Mod. Phys. **80**, 517 (2008).
[18] P. Zanardi, Phys. Rev. A **65**, 042101 (2002).
[19] D. Larsson and H. Johannesson, Phys. Rev. A **73**, 042320 (2006).
[20] A. Osterloh, L. Amico, G. Falci, and R. Fazio, Nature (London) **416**, 608 (2002).
[21] A. Kopp, X. Jia, and S. Chakravarty, Ann. Phys. **322**, 1466 (2007).
[22] S. J. Gu, S. S. Deng, Y. Q. Li, and H. Q. Lin, Phys. Rev. Lett. **93**, 086402 (2004).
[23] L. Gong and P. Tong, Phys. Rev. B **76**, 085121 (2007).
[24] L. Gong and P. Tong, Phys. Rev. E **74**, 056103 (2006).
[25] P. Jordan and E. Wigner, Z. Phys. **47**, 631 (1928).
[26] E. Fradkin, *Field Theories Of Condensed Matter Systems*, 1st ed. (Addison-Wesley, Redwood City, CA, 1991).